Molecular elimination in photolysis of o - and p -fluorotoluene at 193 nm: Internal energy of HF determined with time-resolved Fourier transform spectroscopy

Sheng-Kai Yang, Suet-Yi Liu, Hui-Fen Chen, and Yuan-Pern Lee

Citation: The Journal of Chemical Physics **123**, 224304 (2005); doi: 10.1063/1.2131072
View online: http://dx.doi.org/10.1063/1.2131072
View Table of Contents: http://scitation.aip.org/content/aip/journal/jcp/123/22?ver=pdfcov
Published by the AIP Publishing

Molecular elimination in photolysis of *o*- and *p*-fluorotoluene at 193 nm: Internal energy of HF determined with time-resolved Fourier transform spectroscopy

Sheng-Kai Yang, Suet-Yi Liu, and Hui-Fen Chen
Department of Chemistry, National Tsing Hua University, Hsinchu 30013, Taiwan

Yuan-Pern Lee[a)]
Department of Applied Chemistry and Institute of Molecular Science, National Chiao Tung University, Hsinchu 30010, Taiwan and Institute of Atomic and Molecular Sciences, Academia Sinica, Taipei 10617, Taiwan

(Received 26 July 2005; accepted 7 October 2005; published online 12 December 2005)

Following the photodissociation of *o*-fluorotoluene [o-$C_6H_4(CH_3)F$] at 193 nm, rotationally resolved emission spectra of HF($1 \leqslant v \leqslant 4$) in the spectral region of 2800–4000 cm^{-1} are detected with a step-scan Fourier transform spectrometer. HF($v \leqslant 4$) shows nearly Boltzmann-type rotational distributions corresponding to a temperature ~1080 K; a short extrapolation from data in the period of 0.5–4.5 μs leads to a nascent rotational temperature of 1130±100 K with an average rotational energy of 9±2 kJ mol^{-1}. The observed vibrational distribution of $(v=1):(v=2):(v=3)=67.6:23.2:9.2$ corresponds to a vibrational temperature of 5330±270 K. An average vibrational energy of $25\pm^{12}_{3}$ kJ mol^{-1} is derived based on the observed population of HF($1 \leqslant v \leqslant 3$) and estimates of the population of HF ($v=0$ and 4) by extrapolation. Experiments performed on *p*-fluorotoluene [p-$C_6H_4(CH_3)F$] yielded similar results with an average rotational energy of 9±2 kJ mol^{-1} and vibrational energy of $26\pm^{12}_{3}$ kJ mol^{-1} for HF. The observed distributions of internal energy of HF in both cases are consistent with that expected for four-center elimination. A modified impulse model taking into account geometries and displacement vectors of transition states during bond breaking predicts satisfactorily the rotational excitation of HF. An observed vibrational energy of HF produced from fluorotoluene slightly smaller than that from fluorobenzene might indicate the involvement of seven-membered-ring isomers upon photolysis. © *2005 American Institute of Physics*. [DOI: 10.1063/1.2131072]

I. INTRODUCTION

Photodissociation dynamics of three-center and four-center molecular eliminations are the subject of extensive study because, even though identical end products might be produced, distributions of internal energy of these products are distinct in each process.[1] We have employed step-scan time-resolved Fourier transform spectroscopy (TR-FTS) to investigate the internal distribution of HX (X=F, Cl, or Br) photofragments produced from these molecular elimination channels upon irradiation at 193 nm of halo compounds, including vinyl halides,[2,3] 2-chloro-1,1-difluoroethene (CF_2CHCl),[4] and fluorobenzene.[5] In previous work we have demonstrated that TR-FTS is more powerful than other techniques such as resonance-enhanced multiphoton ionization (REMPI) or laser-induced fluorescence (LIF) in determining the distributions of internal energy of photodissociation products such as HX and CO.[2–7] In all four-center HX-elimination channels that we have investigated so far, we have found that energy participation into this channel is nonstatistical. A simple modified impulse model based on geometries and displacement vectors of transition states during bond breaking predicts satisfactorily the average rotational energy of HF. As a further extension of an investigation of the photodissociation of fluorobenzene, we studied the photodissociation of *o*-fluorotoluene [$o-C_6H_4(CH_3)F$] and *p*-fluorotoluene [$p-C_6H_4(CH_3)F$] at 193 nm to ascertain whether if the addition of a methyl group to the benzene ring and the position of the methyl group relative to the F atom affect the dissociation dynamics. In the dissociation of *o*-fluorotoluene, HF might be produced via, in addition to the typical four-center elimination channel, a five-center HF-elimination channel involving the methyl group.

Photodissociation of phenyl chlorides, bromides, and iodides in the ultraviolet (UV) region[8–10] involves excitation of nonbonding electrons of the halogen atom to an antibonding orbital, leading to a prompt and direct dissociation of the C–X (X=Cl, Br, and I) bond along the repulsive surface. In contrast, fluorosubstituted benzene and its derivatives show a different mechanism because the excitation of the nonbonding electron of the F atom to the antibonding orbital requires greater energies. Huang *et al.*[11] employed the multimass ion-imaging technique to find that, upon photolysis of C_6H_5F at 193 nm, elimination of HF is the major channel,

[a)]Author to whom correspondence should be addressed. Electronic mail: yplee@mail.nctu.edu.tw

$$C_6H_5F + h\nu \rightarrow C_6H_4 + HF, \quad \Delta H^\circ = 283 \text{ kJ mol}^{-1}, \tag{1a}$$

with a branching ratio greater than 0.9, and elimination of H is a minor channel,

$$C_6H_5F + h\nu \rightarrow C_6H_4F + H, \quad \Delta H^\circ \cong 467 \text{ kJ mol}^{-1}. \tag{1b}$$

We observed IR emission of HF from reaction (1a) and determined the distribution of internal energy of HF under similar photodissociation conditions.[5] Although the *F*-elimination channel is energetically accessible at 193 nm (619 kJ mol^{-1}),

$$C_6H_5F + h\nu \rightarrow C_6H_5 + F, \quad \Delta H^\circ = 534 \text{ kJ mol}^{-1}, \tag{1c}$$

Huang *et al.* found no evidence of this channel.[11]

For photodissociation of *o*-$C_6H_4(CH_3)F$ at 193 nm, several channels are energetically accessible:

$$o\text{-}C_6H_4(CH_3)F + h\nu \rightarrow C_6H_3(CH_3) + HF, \quad \Delta H^\circ \cong 330 \text{ kJ mol}^{-1}, \tag{2a}$$

$$o\text{-}C_6H_4(CH_3)F + h\nu \rightarrow C_6H_4(CH_2) + HF, \quad \Delta H^\circ \cong 400 \text{ kJ mol}^{-1}, \tag{2b}$$

$$o\text{-}C_6H_4(CH_3)F + h\nu \rightarrow C_6H_4F + CH_3, \quad \Delta H^\circ \cong 410 \text{ kJ mol}^{-1}, \tag{2c}$$

$$o\text{-}C_6H_4(CH_3)F + h\nu \rightarrow C_6H_4(CH_2)F + H, \quad \Delta H^\circ \cong 360 \text{ kJ mol}^{-1}, \tag{2d}$$

$$o\text{-}C_6H_4(CH_3)F + h\nu \rightarrow C_6H_3(CH_3)F \text{ isomers} + H, \quad \Delta H^\circ \cong 460 \text{ kJ mol}^{-1}, \tag{2e}$$

$$o\text{-}C_6H_4(CH_3)F + h\nu \rightarrow C_6H_4(CH_3) + F, \quad \Delta H^\circ \cong 510 \text{ kJ mol}^{-1}. \tag{2f}$$

Because information on experimental enthalpies of formation for most heavy photofragments is lacking, enthalpies of reactions (listed in kJ mol^{-1}) were taken from quantum-chemical calculations, to be discussed later. Similar dissociation channels can be written for *p*-$C_6H_4(CH_3)F$. Huang *et al.* employed the multimass ion-imaging technique to investigate photodissociation of *p*-$C_6H_4(CH_3)F$ at 193 nm; their preliminary results indicate that at least three channels participate: fission of C–CH_3, C–F, and a C–H bond in the methyl group.[12]

We report here an investigation of the HF elimination in the photolysis of *o*- and *p*-fluorotoluene at 193 nm with time-resolved Fourier transform spectroscopy and compare the observed distribution of internal energy of HF with other similar four-center HF photoeliminations.

II. EXPERIMENTS

The apparatus employed to obtain step-scan time-resolved Fourier transform spectra has been described previously.[4,13,14] The size of the photolysis beam from an ArF laser at 193 nm (Lambda Physik, OPTex) was ~3 $\times 4$ mm^2 at the detection center with a fluence ~35 mJ cm^{-2}. We employed an InSb detector with a rise time of 0.7 μs, and its transient signal was preamplified with a gain factor of 10^5 V A^{-1} (bandwidth of 1.5 MHz), followed by further amplification by a factor of 200 (bandwidth of 1 MHz) before being digitized with an external data-acquisition board [12-bit analog-to-digital converter (ADC)] at 50-ns resolution. Data were typically averaged over 60 laser pulses at each scan step; 2166 scan steps were performed to yield an interferogram resulting in a spectrum of resolution of 2.0 cm^{-1} in the spectral region of 2600–4500 cm^{-1}. To improve the signal-to-noise (S/N) ratio of the spectrum, 20 consecutive time-resolved spectra were subsequently summed to yield spectra representing emission at intervals of 1.0 μs. The temporal instrument response function was determined using an IR laser beam as a source, as described previously.[5]

Fluorotoluene was injected into the vacuum chamber as a diffusive beam through a slit-shaped inlet. The vapor pressures of *o*-$C_6H_4(CH_3)F$ and *p*-$C_6H_4(CH_3)F$ at 298 K are ~24 and 21 Torr, respectively; their partial pressures in the chamber were maintained under 0.021 and 0.030 Torr. The absorption cross sections of *o*-$C_6H_4(CH_3)F$ and *p*-$C_6H_4(CH_3)F$ at 193 nm were determined to be roughly 1.9 and 1.7×10^{-17} cm^2 $molecule^{-1}$, respectively, using a laser power meter.

Ar (Scott Specialty Gases, 99.999%) in a minimal amount was added near the entrance of the photolysis port to suppress the formation of a solid deposit on the quartz window. With Ar purging, the pressure of the system was maintained at ~50 mTorr. *o*-$C_6H_4(CH_3)F$ and *p*-$C_6H_4(CH_3)F$ (both Acros, 99%) were used without purification except for degassing; no impurity was detected in their IR spectra.

III. RESULTS AND ANALYSIS

To maintain a nearly collisionless condition within a 1.0-μs period, the partial pressures of fluorotoluene and Ar were reduced as much as practicable while maintaining a satisfactory signal-to-noise ratio. With an excimer laser at 193 nm, we irradiated *o*- or *p*-$C_6H_4(CH_3)F$ and Ar in a flowing mixture. An investigation of the dependence of signal intensity on the fluence of the photolysis laser indicates that the signal intensity deviated from linearity when the laser fluence was greater than 40 mJ cm^{-2}. Although we are unable to exclude completely the slight possibility of production of HF from fragmentation of molecular ions that might be produced via a 1+1 REMPI process, we believe that such a contribution is negligible based on the results from separate experiments using photofragmentation translational spectroscopy (to be published).

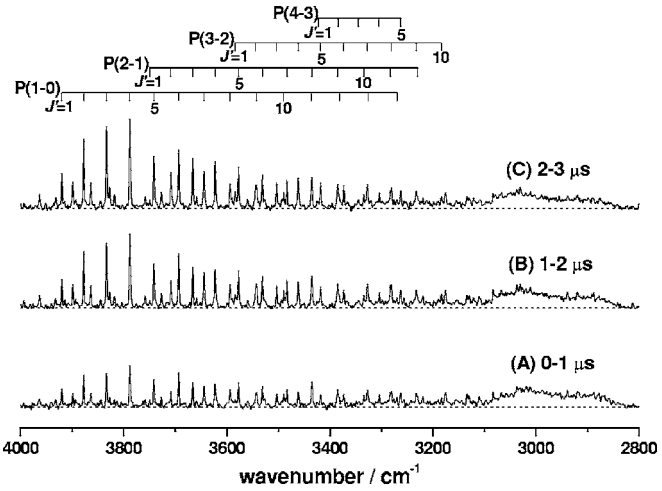

FIG. 1. Infrared emission spectra of HF in spectral region 2800–4000 cm^{-1} recorded at varied intervals after the photolysis of *o*-$C_6H_4(CH_3)F$ (0.021 Torr) in Ar (0.029 Torr) at 193 nm. (A) 0.0–1.0 μs; (B) 1.0–2.0 μs; (C) 2.0–3.0 μs. Spectral resolution is 2.0 cm^{-1}; 60 laser pulses were averaged at each scan step of the interferometer. Assignments are shown as stick diagrams.

A. Photodissociation of *o*-fluorotoluene

1. Infrared emission of HF

Figure 1 shows the partial emission spectra of HF, at a resolution of 2.0 cm^{-1}, recorded 0.0–1.0, 1.0–2.0, and 2.0–3.0 μs after photolysis of a flowing mixture of *o*-$C_6H_4(CH_3)F$ and Ar with partial pressures of 0.021 and 0.029 Torr, respectively; the time has been corrected for instrument response. The partial pressure of the sample in the photolysis region near the exit of the slit is likely greater than the average pressure determined downstream. The smaller intensity in periods of 0.0–1.0 μs reflects the slow rate of production of HF; the temporal evolution of the signal is discussed later. Assignments based on the spectral parameters reported by Sengupta *et al.*[15] and Ram *et al.*[16] are shown as stick diagrams in Fig. 1; values of J' are indicated. The spectrum exhibits emission from HF with J' up to 14 and v up to 4. Each vibration-rotational line was normalized with the instrument response function, and divided by its respective Einstein coefficient[17] to yield a relative population $P_v(J')$. Partially overlapped lines, such as $J'=9,11,12$ of HF($v=1$), $J'=3,8,9,11$ of HF($v=2$), $J'=2,7,8$ of HF($v=3$), and $J'=2,7,9$ of HF($v=4$), were deconvoluted to yield their intensities. Lines associated with $J'=1$ and 5 of HF($v=1$) and $J'=1$ of HF($v=2$ and 3) were not used because of the interference from absorption of ambient air containing some H_2O. Semilogarithmic plots of $P_v(J')/(2J'+1)$ versus rotational energy E_{rot} for HF($v=1$–3) produced from *o*-$C_6H_4(CH_3)F$ are shown in Fig. 2; as only three data points are available for $v=4$, a reliable fit is impracticable. Although the rotational distribution is not exactly Boltzmann, we still assume a Boltzmann distribution for HF in all vibrational levels for a correction of rotational quenching. Fitted Boltzmann-type rotational distributions of HF, derived from the spectrum recorded in the range of 0.0–1.0 μs, yield rotational temperatures of $1070\pm40, 1110\pm50$, and 1070 ± 80 K for $v=1$–3, respectively; unless specified, error limits listed in this paper represent one standard deviation in fitting. Similar procedures were performed for spectra averaged over 1.0–2.0, 2.0–3.0, and 3.0–4.0 μs. With a short extrapolation, we estimate the nascent rotational temperature to be $1120\pm50, 1140\pm40$, and 1130 ± 130 K for $v=1$–3, respectively; an average rotational temperature of 1130 ± 80 K is thus derived.

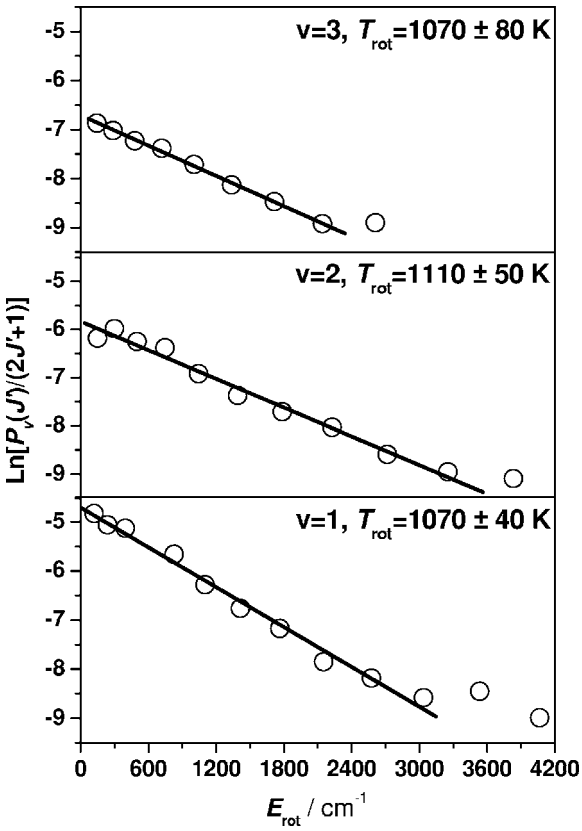

FIG. 2. Semilogarithmic plots of relative rotational populations of HF($v=1$–4) after the photolysis of *o*-$C_6H_4(CH_3)F$ (0.021 Torr) with Ar (0.029 Torr) at 193 nm. Solid lines represent least-squares fits.

We fitted the rotational distribution with a non-Boltzmann function and associated an interpolated population with the missing data. Relative populations obtained on counting levels up to observed J_{max} in each vibrational level (referred as "observed data" hereafter) are indicated as $\Sigma_J P_v(J)$. We normalized the values of $\Sigma_J P_v(J)$ associated with each vibrational state to yield a relative vibrational population $(v=1):(v=2):(v=3)=(67.6\pm7.0):(23.2\pm3.0):(9.2\pm0.9)$, corresponding to a vibrational temperature of 5330 ± 270 K. Rotational energies for each vibrational level, $E_r(v)$, obtained on summing a product of rotational level energy and normalized population for each rotational level, are listed in Table I. An average rotational energy $E_r=8.2\pm1.6$ kJ mol^{-1} for HF($v=1$–3) observed 0.0–1.0 μs after photolysis is derived on summing a product of vibrational population and associated $E_r(v)$. After applying a correction factor $1130/1080=1.05$ for rotational quenching, we derive a nascent rotational energy of 9 ± 2 kJ mol^{-1} based on the observed data.

The highest level of HF observed, $J'=5$ of $v=4$, has an energy 15 357 cm^{-1} above the ground vibrational level; this energy corresponds to $J_{max}(v)=24$, 19, and 14 for $v=1$–3,

TABLE I. Fitted rotational temperature, rotational energy, and vibrational population of HF(v) recorded 0.0–1.0 μs after photolysis of o-$C_6H_4(CH_3)F$ at 193 nm.

v	T_{rot}/K	$E_r(v)$/kJ mol^{-1}	Vibrational population[a]
0			0.653[b] (0.644)[c]
1	1070±40	8.4[b] (8.9)[c]	0.227 (0.230)
2	1110±50	8.2 (9.2)	0.078 (0.080)
3	1070±80	6.8 (7.9)	0.031 (0.033)
4			0.012 (0.013)
Ave.	1080±60	8.2 (8.8)	

[a]Normalized to $v=0$–4; populations of $v=0$ are estimated from extrapolation.
[b]Observed data. Only levels below observed J_{max} in each vibrational level are included; see text.
[c]Extrapolated data are listed parenthetically. All levels up to $E=15\,357$ cm^{-1} above the ground level are included; see text.

respectively. We associate an extrapolated population with unobserved lines up to $J_{max}(v)$ for each vibrational level using the fitted non-Boltzmann distribution to derive a revised population distribution, referred to as "extrapolated data" hereafter; the rotational energies $E_r(v)$ thus derived are listed in parentheses in Table I. An average rotational energy of 8.8±1.8 kJ mol^{-1} and a nascent rotational energy of $E_r=9\pm2$ kJ mol^{-1} estimated with correction for quenching are thus derived from the extrapolated data. The extrapolated data yield a nascent rotational energy similar to that from the observed data; hence we report an average rotational energy of HF as 9±2 kJ mol^{-1}.

Assuming a Boltzmann vibrational distribution, we estimate the population of $v=0$ and 4 relative to $v=1$ to be 2.87 (2.79) and $v=4$ to be 0.05 (0.05) for the observed (extrapolated) data, respectively. The vibrational distribution of HF normalized for $v=0$–4 is thus $(v=0):(v=1):(v=2):(v=3):(v=4)=65.3$: 22.7: 7.8: 3.1: 1.2 and 64.4: 23.0: 8.0: 3.3: 1.3 for the observed and extrapolated data, respectively, as shown in Table I; because the differences in vibrational temperatures between the observed and extrapolated data, 5330±270 K and 5460±280 K, are negligible, only the distribution derived from the observed data is shown in Fig. 3.

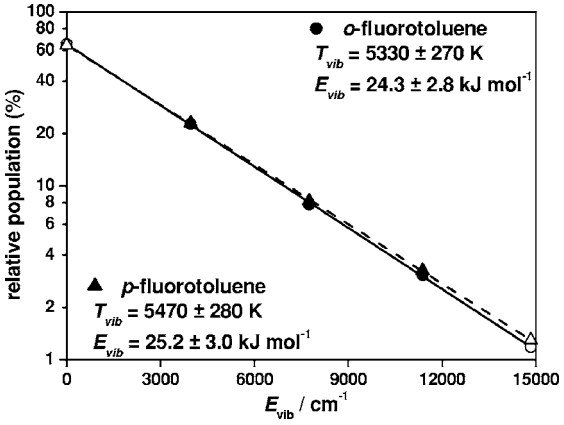

FIG. 3. Relative vibrational distributions of HF($v=0$–4) after the photolysis of o-$C_6H_4(CH_3)F$ (0.021 Torr) in Ar (0.029 Torr) and p-$C_6H_4(CH_3)F$ (0.030 Torr) with Ar (0.045 Torr) at 193 nm. ●: o-$C_6H_4(CH_3)F$; ▲: p-$C_6H_4(CH_3)F$.

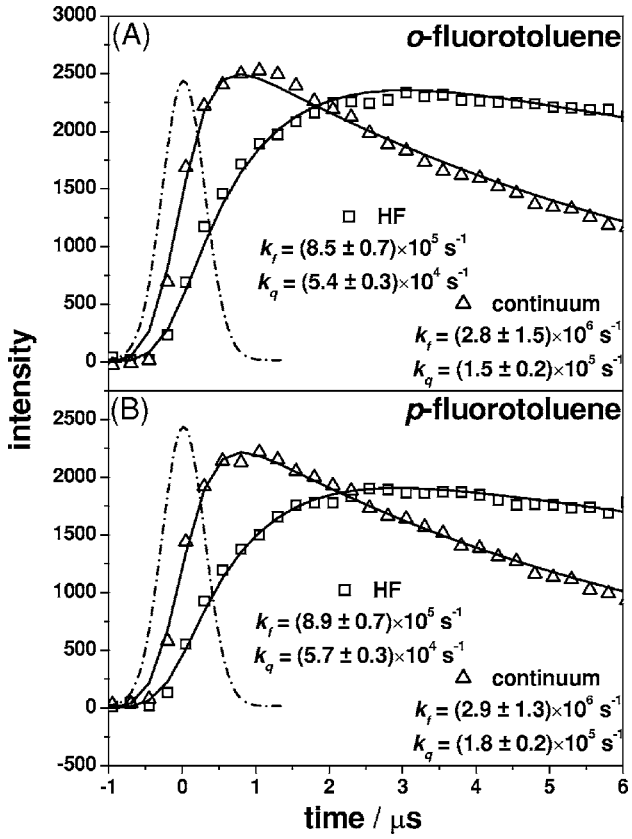

FIG. 4. Temporal profiles of HF (□) and the continuum in a region 2850–3450 cm^{-1} (△) after the photolysis of (A) o-$C_6H_4(CH_3)F$ (0.013 Torr) with Ar (0.022 Torr) and (B) p-$C_6H_4(CH_3)F$ (0.030 Torr) with Ar (0.045 Torr) at 193 nm. The instrument response function is shown in dotted line.

The average vibrational energies of HF derived from the observed and extrapolated data are $E_v=25\pm3$ kJ mol^{-1}.

If the vibrational population has a smooth non-Boltzmann distribution, we might estimate a lower bound of the population of $v=0$ to be 1.3 times that of $v=1$. The average vibrational energy of $E_v=37$ kJ mol^{-1} thus derived might be taken as an upper limit. Taking this upper limit into account, we report an average vibrational energy of HF as $25\pm^{12}_{3}$ kJ mol^{-1}.

A weak continuous emission in the range of 2800–3400 cm^{-1} was present at an early stage ($t\leqslant5$ μs) after irradiation (Fig. 1) and diminished after $t\geqslant20$ μs; the lower bound of the spectrum might be limited by the transmission of the IR filter. With the present detectivity and resolution, we are unable to assign positively the carrier of this broad feature. Possible candidates are the emissions from the parent or fragments such as $C_6H_4(CH_2)F$, $C_6H_3(CH_3)F$, $C_6H_4(CH_3)$, $C_6H_3(CH_3)$, or C_6H_4F; emission of internally hot parent also contributes to part of this continuous emission.

2. Temporal profiles of emission

The temporal evolution of emission of HF and the broad feature produced from the photolysis of o-$C_6H_4(CH_3)F$ (0.021 Torr) with Ar (0.029 Torr) at 193 nm are shown in Fig. 4(A). The total intensity for emission of the broad feature was derived by integration of the spectrum with features

TABLE II. Calculated H–F length R_{HF}, torque angle α, total available energy E_{ava}, exit barrier E_{exit}, and E_{rot} of HF from of o-$C_6H_4(CH_3)F$ and p-$C_6H_4(CH_3)F$ predicted with revised impulse model [calculated with B3LYP/6-311G(d,p)].

Transition state	R_{HF} (Å)	α (deg)	E_{avail} (kJ mol^{-1})	E_{exit} (kJ mol^{-1})	E_{rot} (kJ mol^{-1})
o-TS4	1.09	27.0°	291	54	9.7
o-TS5	0.99	50.8°	219	59	31
o-TS7-4B	1.17	8.0°	239	89	1.5
o-TS7-4A	1.23	9.2°	321	142	3.2
p-TS3	1.55	3.1°	247	157	0.4
p-TS4	1.08	29.0°	247	55	11.3
p-TS7-4	1.23	9.2°	325	142	3.2

associated with HF subtracted at each time interval, whereas that of HF was derived by integration of lines with the broad feature removed. Emission of the broad feature reaches a maximum at ~0.7 μs, whereas that of HF reaches a maximum at ~2 μs. We deconvoluted these profiles with the instrument response function (shown as dot-dashed lines in Fig. 4) and modeled them with a mechanism consisting of formation and quenching in first order to derive rates of formation $k_f=(8.5\pm0.7)\times10^5$ and $(2.8\pm1.5)\times10^6$ s^{-1} and rates of quenching $k_q=(5.4\pm0.3)\times10^4$ and $(1.5\pm0.2)\times10^5$ s^{-1} for HF and the broad feature, respectively. Considering the error associated with the intensity of the broad feature, the deviation in rates of production might not be significant. Nevertheless, a smaller rate of production of HF might indicate that only a portion of the trajectory satisfying a certain geometry constraint can proceed to produce HF whereas emission of parent or fragments produced from other channels has less constraint.

3. Calculations on transition states of *o*-$C_6H_4(CH_3)F$ and branching ratios

We performed calculations to optimize structures of transition states for four-center (*o*-TS4) and five-center (*o*-TS5) elimination channels of *o*-$C_6H_4(CH_3)F$ and transition states involving a seven-membered ring (*o*-TS7A, *o*-TS7B, *o*-TS7-4A, and *o*-TS7-4B) with the B3LYP/6-311G(d,p) density-functional theory[18,19] using the GAUSSIAN03 program.[20] predicted H–F bond lengths of transition states *o*-TS4, *o*-TS5, *o*-TS7-4A, and *o*-TS7-4B and the torque angles associated with the motion of the dissociating H atom toward the F atom in the imaginary vibrational mode are summarized in Table II. Relative energies and barriers of these HF-elimination channels are shown in Fig. 5(A). The energies of the HF-elimination channels were further calculated with the CCSD/6-311++G(d,p) method at geometries optimized with B3LYP for comparison. Calculations using the B3LYP method yield barriers of 382 and 459 kJ mol^{-1}, whereas those with the CCSD method yield 428 and 516 kJ mol^{-1} for four-center and five-center elimination channels via transition states *o*-TS4 and *o*-TS5, respectively. Unless noted, we state in this section only energies calculated with B3LYP/6-311G(d,p). Additional four-center elimination channels proceed via a transition state *o*-TS7A with a barrier of 355 kJ mol^{-1} to form a seven-membered-ring *o*-LM7A, which readily converts to another isomer *o*-LM7B with energy about 141 kJ mol^{-1} above *o*-$C_6H_4(CH_3)F$; subsequent four-center HF-elimination channels proceeds via either *o*-TS7-4A or *o*-TS7-4B with barriers of 441 or 469 kJ mol^{-1}, respectively. Relative energies and barriers of seven simple bond-fission channels are

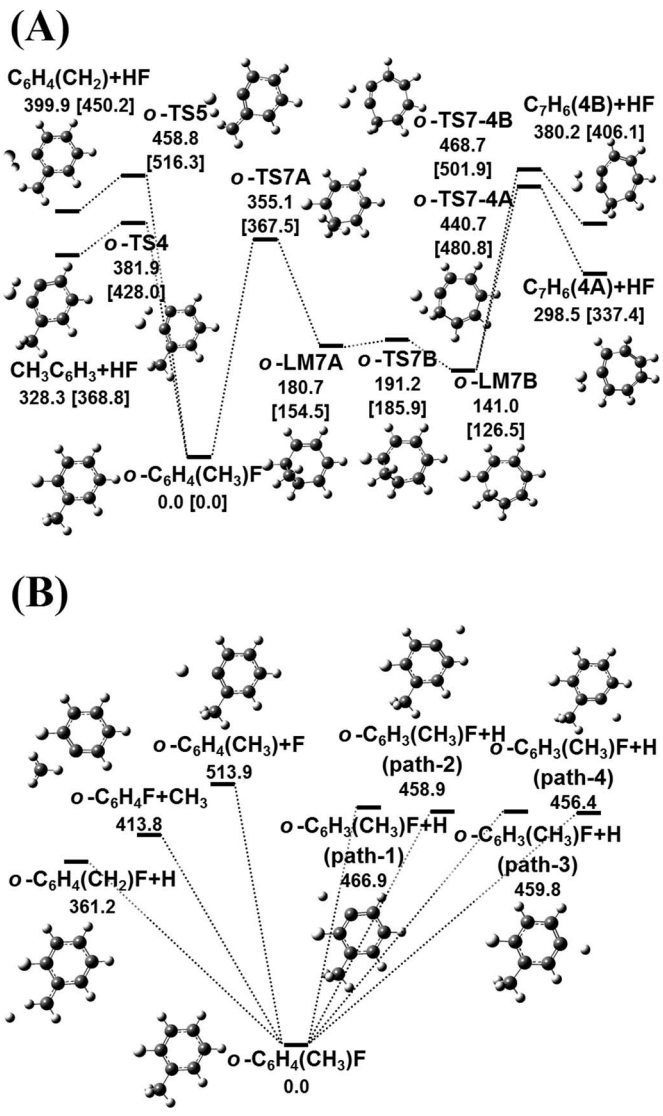

FIG. 5. Energy (in kJ mol^{-1}) of various dissociation channels of *o*-$C_6H_4(CH_3)F$ calculated with B3LYP/6-311G(d,p). Energies predicted with CCSD/6-311++G(d,p)//B3LYP/6-311G(d,p) are listed in parentheses. (A) HF-elimination; (B) simple bond fission.

shown in Fig. 5(B). The two channels requiring the least energy are fission of the C–H bond of the methyl group (361 kJ mol^{-1}) and fission of the $C–CH_3$ bond (414 kJ mol^{-1}).

We estimated rates of dissociation via these four possible HF-elimination channels on the ground electronic surface of *o*-$C_6H_4(CH_3)F$ with a Rice-Ramsperger-Kassel-Marcus (RRKM) theory. The Whitten-Rabinovitch equations[21] were used to calculate the density of states. Using barriers and vibrational wave numbers calculated with B3LYP/6-311G(*d*,*p*), we calculated rate coefficients for HF-elimination channel via four-center (*o*-TS4), five-center (*o*-TS5), and four-center transition states after initial formation of a seven-membered ring (*o*-TS7-4A and *o*-TS7-4B) to be 3.6×10^4, 13, 5.2×10^3, and 61 s^{-1}, respectively; the latter two were derived on assuming a steady state of seven-membered-ring intermediates. Accordingly, the production of HF via four-center elimination on the ground electronic surface is expected to dominate.

B. Photodissociation of *p*-fluorotoluene

For similar experiments and calculations performed for *p*-$C_6H_4(CH_3)F$, we present only brief descriptions as follows.

1. Infrared emission of HF

Emission spectra of HF, at a resolution of 2.0 cm^{-1}, upon photolysis of a flowing mixture of *p*-$C_6H_4(CH_3)F$ and Ar with partial pressures of 0.030 and 0.045 Torr are similar to those observed for photolysis of *o*-$C_6H_4(CH_3)F$. The spectrum exhibits emission from HF with J' up to 14 and v up to 4. Semilogarithmic plots of $P_v(J')/(2J'+1)$ vs $E_{\rm rot}$ for HF(v=1–3) produced from *p*-$C_6H_4(CH_3)F$ are shown in Fig. 6. The rotational distribution of HF also deviates slightly from a Boltzmann distribution. Fitted Boltzmann-type rotational distributions of HF, derived from the spectrum recorded in the range of 0.0–1.0 μs, yield rotational temperatures of 1070±40, 1120±50, and 1070±130 K for v=1–3, respectively. With a short extrapolation, we estimate an average rotational temperature of 1140±80 K for nascent HF.

An average rotational energy E_r=8.2±1.6 kJ mol^{-1} for HF(v=1–3) observed of 0.0–1.0 μs after photolysis is derived on summing a product of vibrational population and associated $E_r(v)$. After applying a correction factor of 1140/1090=1.05 for rotational quenching, we derive a nascent rotational energy of 9±2 kJ mol^{-1} based on the observed data. Nearly identical results are derived from the extrapolated data.

Assuming a Boltzmann vibrational distribution, we derived a vibrational distribution of HF normalized for v=0–4, as $(v=0):(v=1):(v=2):(v=3):(v=4)$=64.3: 22.9: 8.2: 3.3: 1.3 and 62.9: 23.5: 8.5: 3.6: 1.5 for the observed and extrapolated data, respectively, as shown in Table III; as the differences in vibrational temperatures between the observed and extrapolated data, 5470±280 and 5680±280 K, are negligible, only the distribution derived from the observed data is shown in Fig. 3. The average vibrational energy of HF is E_v=26±3 kJ mol^{-1}.

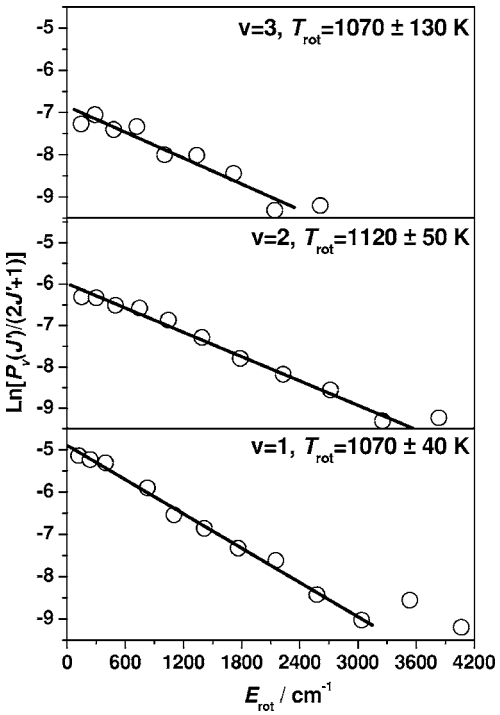

FIG. 6. Semilogarithmic plots of relative rotational populations of HF(v=1–4) after the photolysis of *p*-$C_6H_4(CH_3)F$ (0.030 Torr) with Ar (0.045 Torr) at 193 nm. Solid lines represent least-squares fits.

If the vibrational population has a smooth non-Boltzmann distribution, we can estimate a lower bound of the population of v=0 to be 1.3 times that of v=1. The average vibrational energy of E_v=38 kJ mol^{-1} thus derived might be taken as an upper limit. Taking this upper limit into account, we report an average vibrational energy of HF as $26\pm^{12}_{3}$ kJ mol^{-1}.

2. Temporal profiles of emission

The temporal evolution of emission of HF and the broad feature produced from photolysis of *p*-$C_6H_4(CH_3)F$ at 193 nm are shown in Fig. 4(B). Emission of the broad feature reaches a maximum at ~0.7 μs, whereas that of HF reaches a maximum at ~2 μs. We derived rates of formation k_f $=(8.9\pm0.7)\times10^5$ and $(2.9\pm1.3)\times10^6$ s^{-1} and rates of

TABLE III. Fitted rotational temperature, rotational energy, and vibrational population of HF(v) recorded 0.0–1.0 μs after photolysis of *p*-$C_6H_4(CH_3)F$ at 193 nm.

v	$T_{\rm rot}$/K	$E_r(v)$/kJ mol^{-1}	Vibrational population[a]
0			0.643[b] (0.629)[c]
1	1070±40	8.4[b] (8.9)[c]	0.229 (0.235)
2	1120±50	8.2 (9.3)	0.082 (0.085)
3	1070±130	6.8 (8.7)	0.033 (0.036)
4			0.013 (0.015)
Ave.	1090±80	8.2 (8.9)	

[a]Normalized to v=0–4. Populations of v=0 are estimated from extrapolation.
[b]Observed data. Only levels below observed $J_{\rm max}$ in each vibrational level are included; see text.
[c]Extrapolated data are listed parenthetically. All levels up to E =15 357 cm^{-1} above the ground level are included; see text.

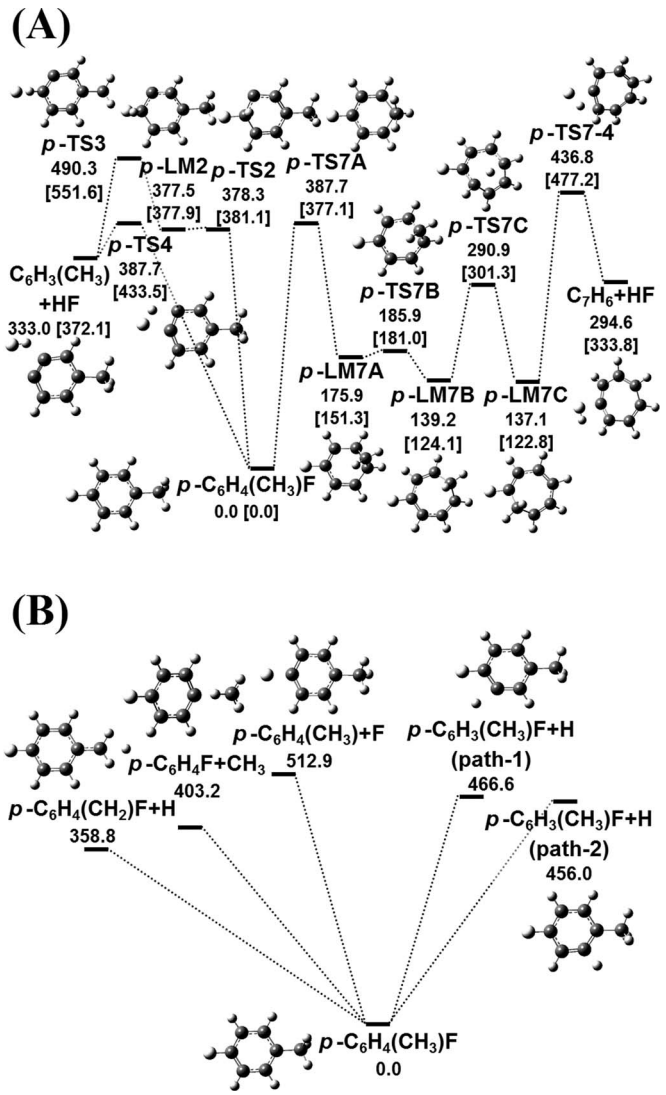

FIG. 7. Energy (in kJ mol^{-1}) of various dissociation channels of p-$C_6H_4(CH_3)F$ calculated with B3LYP/6-311G(d,p). Energies predicted with CCSD/6-311++G(d,p)//B3LYP/6-311G(d,p) are listed in parentheses. (A) HF-elimination; (B) simple bond fission.

quenching $k_q=(5.7\pm0.3)\times10^4$ and $(1.8\pm0.2)\times10^5$ s^{-1} for HF and the broad feature, respectively, similar to the photolysis of o-$C_6H_4(CH_3)F$.

3. Calculations on transition states of p-$C_6H_4(CH_3)F$ and branching ratios

We performed calculations to optimize structures of transition states for four-center (p-TS4) and three-center (p-TS3) elimination channels of p-$C_6H_4(CH_3)F$ and transition states involving a seven-membered ring (p-TS7A, p-TS7B, p-TS7C, and p-TS7-4) with B3LYP/6-311G(d,p). The predicted H–F bond lengths of transition states p-TS4, p-TS3, and p-TS7-4 and the torque angles associated with the motion of the dissociating H atom toward the F atom in the imaginary vibrational mode are summarized in Table II. Relative energies and barriers of these HF-elimination channels, calculated with B3LYP/6-311G(d,p) and CCSD/6-311++G(d,p) are shown in Fig. 7(A). Calculations using the B3LYP method yield barriers of 388 and 490 kJ mol^{-1} for four-center and three-center elimination channels via transition states p-TS4 and p-TS3, respectively. An additional channel proceeds via seven-membered-ring transition states and a subsequent H shift before the four-center HF-elimination channel via the p-TS7-4 transition state with a barrier of 437 kJ mol^{-1}. Relative energies and barriers of five simple bond-fission channels are shown in Fig. 7(B). The two channels requiring the least energy are fission of a C–H bond of the methyl group (359 kJ mol^{-1}) and fission of the C–CH_3 bond (403 kJ mol^{-1}).

We estimated rates of dissociation via these three possible HF elimination channels of p-$C_6H_4(CH_3)F$ with the RRKM theory. Rate coefficients for HF elimination via four-center (p-TS4), three-center (p-TS3), and four-center transition states after initial formation of a seven-membered ring (p-TS7-4) are 1.1×10^4, 0.29, and 18 s^{-1}, respectively; the latter two values were derived on assuming steady-state conditions for reaction intermediates. Accordingly, production of HF via four-center elimination on the ground electronic surface is expected to dominate.

IV. DISCUSSION

In these experiments we were able to use a total pressure less than 0.075 Torr and employed a data acquisition window with a width of 1.0 μs so that the observed rotational quenching was nearly negligible. As discussed previously, the correction to rotational temperature due to quenching is only ~5%. Vibrational quenching is negligible under our experimental conditions. According to the RRKM calculations, HF is produced mainly via the four-center elimination channel of fluorotoluene. The distribution of internal energy of HF observed in this work is consistent with such a model, as discussed below.

A. Rotational energy of HF

Our previous experiments[2,3] indicate that the average rotational energy of HF produced via four-center elimination might be rationalized with a revised impulse model. Assuming that the H atom receives most of the available energy, we distributed the available energy between H and C atoms during bond breaking, followed by calculations of rotational energy of HF according to classical mechanics. Instead of assuming that the H atom moves along the direction of the breaking bond as in a standard impulse model, we considered the direction of motion of the H atom to follow the displacement vector associated with the imaginary vibrational mode of the transition state. Rotational energies are predicted with this modified impulse model according to the equation

$$E_{\rm rot}=[m_F m_C/(m_H+m_F)(m_H+m_C)]E_{\rm exit}\sin^2\alpha, \qquad (3)$$

in which $E_{\rm exit}$ is the exit barrier and α is the torque angle between the direction of motion of H and that of the H–F bond. With exit barriers of 54 and 59 kJ mol^{-1} and $\alpha=27.0°$ and 50.8 ° predicted for four-center and five-center elimination channels of o-$C_6H_4(CH_3)F$, respectively, rotational energies of 9.7 and 31 kJ mol^{-1} are predicted. The former is nearly identical to the experimental value of

TABLE IV. Comparison of total available energy, calculated exit barrier, H–F length R_{HF}, and torgue angle α of TS4, observed average internal energies, and rotational energies of HF predicted with a revised impulse model. (All energies are in unit of kJ mol^{-1}. E_v: vibrational energy; E_r: rotational energy.)

Species	E_{ava}	E_{exit}	R_{HF} (Å)	α (deg)	E_v (expt)	E_r (expt)	E_r (impulse)[a]	Ref.
CH_2CHF	528	219	1.28	8.2	83±9	2.5±1.5[b]	3.9	3 and 24
CF_2CHCl	458	199	1.18	17.5	46±6	20±4	15.8	4
C_6H_5F	284	56	1.08	32.8	$33\pm^{9}_{3}$	15±3	15.4	5
o-$C_6H_4(CH_3)F$	250	54	1.09	27.0	$25\pm^{12}_{3}$	9±2	9.7	This work
P-$C_6H_4(CH_3)F$	247	55	1.08	29.0	$26\pm^{12}_{3}$	9±2	11.3	This work

[a]Assuming that the motion of H atom is along the displacement vector corresponding to the imaginary mode of the transition state; see text.
[b]Trajectory calculations (Ref. 24) indicate that the four-center elimination channel produces high-*J* components; see text.

9 ± 2 kJ mol^{-1}. Considering possible errors associated with the exit barrier and the relatively simple impulse model, the agreement is satisfactory. The average rotational energy of 9 ± 2 kJ mol^{-1} for HF implies that a small fraction of total available energy, $f_r \cong 0.038\pm0.008$, is partitioned into HF upon dissociation of *o*-$C_6H_4(CH_3)F$ at 193 nm.

Similarly, E_{exit}, torque angle α, and E_{rot} predicted with the revised impulse model for three possible HF-elimination channels of *p*-$C_6H_4(CH_3)F$ are listed in Table II. With available energies of 55 kJ mol^{-1} and $\alpha=29.0°$ predicted for *p*-TS4 of *p*-$C_6H_4(CH_3)F$, a rotational energy of 11.3 kJ mol^{-1} is predicted, near the experimental value of 9 ± 2 kJ mol^{-1}.

B. Vibrational energy of HF

The disadvantage of the infrared emission technique is the lack of information on the $v=0$ level. Even though we do not expect extensive vibrational excitation for HF based on the theoretical predictions to be discussed below, experimentally we cannot positively exclude the possibility of a non-Boltzmann vibrational distribution; the upper error limit is hence much greater than expected. The average vibrational energies of $25\pm^{12}_{3}$ and $26\pm^{12}_{3}$ kJ mol^{-1} for HF from *o*-$C_6H_4(CH_3)F$ and *p*-$C_6H_4(CH_3)F$, respectively, imply that a moderate fraction of available energy is partitioned into HF, with $f_v \cong 0.10\pm^{0.05}_{0.01}$. The partition of vibrational energy is expected to depend on the deviation of the distance between two bond-forming atoms from their equilibrium distance. Predicted distances between H and F are 1.09, 0.99, 1.17, and 1.23 Å for *o*-TS4, *o*-TS5, *o*-TS7-4B, and *o*-TS7-4A in dissociation of *o*-$C_6H_4(CH_3)F$ and 1.55, 1.08, and 1.23 Å for *p*-TS3, *p*-TS4, and *p*-TS7-4 in dissociation of *p*-$C_6H_4(CH_3)F$, respectively (Table II). Because the equilibrium bond distance of HF is 0.9168 Å (Ref. 22), one would expect that the vibrational excitation of HF produced from *o*-$C_6H_4(CH_3)F$ via *o*-TS4 and *o*-TS5 is smaller than that via *o*-TS7-4A and *o*-TS7-4B. As a comparison, R_{HF} in TS4 for four-center elimination of fluorobenzene is predicted to be 1.08 Å and the observed average vibrational energy of HF is $33\pm^{9}_{3}$ kJ mol^{-1}.[5] Hence, the observed vibrational distribution of HF from *o*-$C_6H_4(CH_3)F$ fits satisfactorily with the four-center or five-center elimination mechanism, but not with the four-center elimination mechanism via the seven-membered ring. Similarly, the observed vibrational distribution of HF from *p*-$C_6H_4(CH_3)F$ fits satisfactorily with the four-center elimination mechanism.

C. Rates of production and quenching

Electronic excitation of *o*-$C_6H_4(CH_3)F$ and *p*-$C_6H_4(CH_3)F$ have not been investigated. We expect that HF elimination proceeds via the ground electronic surface, after internal conversion from its initially prepared excited state. After deconvolution of temporal profiles of HF with the instrument response function, we obtained nearly identical rates of formation of $(8.5\pm0.7)\times10^5$ and $(8.9\pm0.7)\times10^5$ s^{-1} for HF from *o*-$C_6H_4(CH_3)F$ and *p*-$C_6H_4(CH_3)F$. These rates of formation are similar to that, $(1.0\pm0.3)\times10^6$ s^{-1}, determined for HF upon irradiation of fluorobenzene at 193 nm.[5] Rates of formation of HF via the four-center elimination channels of *o*-$C_6H_4(CH_3)F$ and *p*-$C_6H_4(CH_3)F$ are predicted with the RRKM theory to be 3.6×10^4 and 1.1×10^4 s^{-1}, respectively, about 1%–5% of those determined experimentally. The deviation between experimental and calculation results is unclear; one possible reason might be errors in calculated energies.

Observed rates of quenching for HF, $(5.4\pm0.3)\times10^4$ s^{-1} at $[o\text{-}C_6H_4(CH_3)F]=6.8\times10^{14}$ molecule cm^{-3} and $(5.7\pm0.3)\times10^4$ s^{-1}, at $[p\text{-}C_6H_4(CH_3)F]=9.7\times10^{14}$ molecule cm^{-3}, imply apparent bimolecular rate coefficients for vibrational quenching $k_q^{II}=8\times10^{-11}$ cm^3 molecule^{-1} s^{-1} by *o*-$C_6H_4(CH_3)F$ and $k_q^{II}=6\times10^{-11}$ cm^3 molecule^{-1} s^{-1} by *p*-$C_6H_4(CH_3)F$; vibrational quenching of HF by Ar is much smaller and can therefore be ignored.[23] These rate coefficients for quenching are similar to a value $(6.3\pm0.5)\times10^{-11}$ cm^3 molecule^{-1} s^{-1} determined for fluorobenzene;[5] they represent mainly quenching from the $v=1$ state of HF. We did not study the detailed rates of quenching for each individual vibrational state.

D. Comparison with photolysis of various fluorocompounds

The observed rotational energies of HF from four-center elimination channels of CH_2CHF,[3] CF_2CHCl,[4] C_6H_5F,[5] *o*-$C_6H_4(CH_3)F$, and *p*-$C_6H_4(CH_3)F$ are compared in Table IV. Although the total available energies and the exit barriers

for these five systems vary substantially, the observed rotational energies of HF agree satisfactorily with those predicted with the modified impulse model. In contrast, recent trajectory calculations indicate that the rotational excitation of HF produced from the four-center elimination of CH_2CHF produces more rotationally excited HF than the three-center elimination channel.[24] Further investigations are needed to clarify this discrepancy.

HF produced from CF_2CHCl and C_6H_5F, both via four-center elimination, has similar rotational energy; nevertheless the exit barrier for C_6H_5F is only 56/199=0.28 that for CF_2CHCl. The torque angle for TS4 of CF_2CHCl is nearly half that of C_6H_5F; hence the efficiency of rotational excitation of HF is decreased. The exit barriers for the four-center elimination channels of *o*-$C_6H_4(CH_3)F$ and *p*-$C_6H_4(CH_3)F$ are similar to that of C_6H_5F, but their torque angles are slightly smaller; hence the predicted rotational energies are smaller, consistent with experiments.

Likewise, average vibrational energies of HF via four-center elimination of these molecules are compared in Table IV. CH_2CHF has the largest vibrational-energy partitioning into HF because its predicted bond distance of TS4 is 1.28 Å, much greater than the equilibrium bond distance of HF, 0.9168 Å. Calculated wave functions also indicate that the H–F bond in TS4 of CH_2CHF is not yet "formed."

The nearly identical distributions of internal energy of HF produced from *o*-$C_6H_4(CH_3)F$ and *p*-$C_6H_4(CH_3)F$ indicate that the relative positions of the F atom and the methyl group have little effect on photodissociation dynamics; the five-center elimination channel of *o*-$C_6H_4(CH_3)F$ plays a minor role. The averaged vibrational energy of HF, $\sim 25\pm^{12}_{3}$ kJ mol^{-1}, for photodissociation of both *o*- and *p*-fluorotoluene at 193 nm, is smaller than that observed for HF from photolysis of C_6H_5F, even though the predicted H–F bond lengths of transition states in these three cases are similar. The variation might arise partly because the available energy for dissociation of fluorotoluene is about 17% smaller than that of C_6H_5F. However, the slightly smaller fraction of vibrational-energy partition into HF upon photodissociation of fluorotoluene might indicate that isomerization to seven-membered rings before dissociation plays a role.

V. CONCLUSION

Rotationally resolved emission of HF up to $v=4$ is observed upon photolysis of *o*-$C_6H_4(CH_3)F$ and *p*-$C_6H_4(CH_3)F$ at 193 nm; HF is likely produced from the four-center elimination channel on the ground electronic surface. The average rotational energy of 9 ± 2 kJ mol^{-1} and vibrational energy of $\sim 25\pm^{12}_{3}$ kJ mol^{-1} for HF in both cases implies that a moderate fraction of available energy is partitioned into the internal energy of HF, with $f_v \cong 0.10\pm^{0.05}_{0.01}$ and $f_r \cong 0.038\pm0.008$. A modified impulse model considering displacement vectors of transition states during bond breaking predicts the rotational distributions of HF satisfactorily for four-center elimination channels of CH_2CHF, CF_2CHCl, C_6H_5F, *o*-$C_6H_4(CH_3)F$, and *p*-$C_6H_4(CH_3)F$. Partition of vibrational energy into HF upon photolysis is consistent with distances of H–F predicted for transition states of four-center elimination for these systems; a slightly smaller fraction of vibrational-energy partition for *o*-$C_6H_4(CH_3)F$ and *p*-$C_6H_4(CH_3)F$ might indicate that isomerization to seven-membered ring plays a role.

ACKNOWLEDGMENTS

The authors thank the National Science Council of Taiwan (Grant No. NSC93-2119-M-009-002) for support and the National Center for High-Performance Computing for computer time.

[1] Y.-P. Lee, Annu. Rev. Phys. Chem. **54**, 215 (2003).
[2] S.-R. Lin, S.-C. Lin, Y.-C. Lee, Y.-C. Chou, I-C. Chen, and Y.-P. Lee, J. Chem. Phys. **114**, 160 (2001).
[3] S.-R. Lin, S.-C. Lin, Y.-C. Lee, Y.-C. Chou, I-C. Chen, and Y.-P. Lee, J. Chem. Phys. **114**, 7396 (2001).
[4] C.-Y. Wu, C.-Y. Chung, Y.-C. Lee, and Y.-P. Lee, J. Chem. Phys. **117**, 9785 (2002).
[5] C.-Y. Wu, Y.-J. Wu, and Y.-P. Lee, J. Chem. Phys. **121**, 8792 (2004).
[6] C.-Y. Wu, Y.-P. Lee, J. F. Ogilvie, and N. S. Wang, J. Phys. Chem. A **107**, 2389 (2003).
[7] C.-Y. Wu, Y.-P. Lee, and N. S. Wang, J. Chem. Phys. **120**, 6957 (2004).
[8] A. M. Mebel, M. C. Lin, D. Chakraborty, J. Park, S. H. Lin, and Y. T. Lee, J. Chem. Phys. **114**, 8421 (2001), and references therein.
[9] S.-T. Tsai, C.-L. Huang, Y. T. Lee, and C.-K. Ni, J. Chem. Phys. **115**, 2449 (2001).
[10] C.-K. Lin, C.-L. Huang, J.-C. Jiang, A. H. H. Chang, Y. T. Lee, S. H. Lin, and C.-K. Ni, J. Am. Chem. Soc. **124**, 4068 (2002).
[11] C.-L. Huang, J.-C. Jiang, A. M. Mebel, Y. T. Lee, and C.-K. Ni, J. Am. Chem. Soc. **125**, 9814 (2003).
[12] C.-L. Huang, J.-C. Jiang, S.-H. Lin, Y. T. Lee, and C.-K. Ni, Aust. J. Chem. **54**, 561 (2001).
[13] P.-S. Yeh, G.-H. Leu, Y.-P. Lee, and I-C. Chen, J. Chem. Phys. **103**, 4879 (1995).
[14] S.-R. Lin and Y.-P. Lee, J. Chem. Phys. **111**, 9233 (1999).
[15] U. K. Sengupta, P. K. Das, and K. N. Rao, J. Mol. Spectrosc. **74**, 322 (1979).
[16] R. S. Ram, Z. Morbi, B. Guo, K.-Q. Zhang, P. F. Bernath, J. V. Auwera, J. W. C. Johns, and S. P. Davis, Astrophys. J., Suppl. Ser. **103**, 247 (1996).
[17] E. Arunan, D. W. Setser, and J. F. Ogilvie, J. Chem. Phys. **97**, 1734 (1992).
[18] A. D. Becke, J. Chem. Phys. **98**, 5648 (1993).
[19] C. Lee, W. Yang, and R. G. Parr, Phys. Rev. B **37**, 785 (1988).
[20] M. J. Frisch, G. W. Trucks, H. B. Schlegel *et al.*, GAUSSIAN03, revision A.7 (Gaussian, Inc., Pittsburgh, PA, 2003).
[21] K. A. Holbrook, M. J. Pilling, and S. H. Robertson, *Unimolecular Reactions*, 2nd ed. (Chichester, New York, 1996).
[22] K. P. Huber and G. Herzberg, *Constants of Diatomic Molecules*, Molecular Spectra and Molecular Structure, Vol. IV (van Nostrand, Princeton, 1979).
[23] S. R. Leone, J. Phys. Chem. Ref. Data **11**, 953 (1982), and references therein.
[24] E. Martínez-Núñez and S. A. Vázquez, J. Chem. Phys. **121**, 5179 (2004).